JOURNAL OF SOLID STATE CHEMISTRY 99, 395–403 (1992)

# Protonic Location in Hydrogen Molybdenum Bronzes $H_xMoO_3$ as Studied by Proton NMR Lineshape Analysis

M. KUNITOMO, K. EDA, N. SOTANI, AND M. KABURAGI

*College of Liberal Arts, Kobe University, Turukabuto, Nada, Kobe 657, Japan*

Received June 21, 1991; in revised form October 24, 1991; accepted March 31, 1992

Rigid lattice proton NMR spectra are observed in four types of hydrogen molybdenum bronzes $H_xMoO_3$ with pulsed NMR. Lineshapes of the spectra are analyzed by computer-simulation. We conclude that the spectrum of type I ($0.21 \leqq x \leqq 0.40$) is a superposition of the spectrum originating in a two-spin system (Pake-doublet) and the one originating in a three-spin system. On the other hand, the spectra of types II ($0.85 \leqq x \leqq 1.04$), III ($1.55 \leqq x \leqq 1.72$), and IV ($x \simeq 2.0$) consist of a Pake-doublet, a Gaussian, and a Lorentzian. The Gaussian and the Lorentzian are attributed to isolated and immobile protons, and mobile protons, respectively. From the analyses, portions of hydrogen contents of different locations and distances between nearest neighbor protons are determined for all four types of the bronzes. Transition of the protonic structure from type I to II is discussed. © 1992 Academic Press, Inc.

## Introduction

Recently considerable attention has been focused on the physical and chemical properties of hydrogen molybdenum bronze $H_xMoO_3$ because it is of interest not only from an academic point of view but also in technological applications, such as secondary battery electrodes, hydrogen storage cells and catalyst, etc. (*1*). As is well known, the bronze exhibits four distinct phases with the homogeneity of approximate limits (*2, 3*): type I (blue orthorhombic, $0.21 \leqq x \leqq 0.40$), type II (blue monoclinic, $0.85 \leqq x \leqq 1.04$), type III (red monoclinic, $1.55 \leqq x \leqq 1.72$), and type IV (green monoclinic, $x \simeq 2.0$). These bronzes possess a high metal-like conductivity.

Inserted hydrogen atoms into $MoO_3$ layers are linked to oxygen atoms at vertexes of $MoO_6$ octahedra, or to terminal oxygen atoms of $MoO_6$ octahedra at the van der Waals gaps (*4*). The location and mobility of hydrogens in the bronzes are considered to be most crucial factors for their properties and have been investigated extensively by using inelastic neutron scattering (INS) (*4–8*) and also proton NMR for both the motionally narrowed high-temperature spectra (*9–12*) and the rigid-lattice (dipolar-broadened) low-temperature ones (*12–14*). Above all, the pioneering work by Slade *et al.* (*12*) revealed the presence of proton clusters. However, the rigid-lattice spectra obtained by Slade *et al.* (*12*) and those by Ritter *et al.* (*13, 14*) were inconsistent with each other. Slade *et al.* (*12*) suggested that most protons in type I constitute pairs of OH groups in the form of neighboring hydroxyl hydrogens, whereas those in type III form



0022-4596/92 $5.00
Copyright © 1992 by Academic Press, Inc.
All rights of reproduction in any form reserved.

$OH_2$ groups coordinated to Mo atoms. On the other hand, by comparing the spectra with results of computer-simulation, Ritter *et al.* (*13, 14*) proposed a different model for type I in which hydroxyl hydrogens form three proton clusters. They also discussed the nature of the clustering from a viewpoint of charge transfer together with that of isolated protons. Although certain differences in the results of various authors may be caused by the specific samples and different preparation manners, the protonic location in type I is, we believe, still unsettled.

Recently we investigated rigid-lattice spectra to resolve the above contradiction and obtained them in all four phases of the bronzes. In the previous preliminary report (*15*), we have clearly shown that the spectra of types II–IV are superpositions of a Pake-doublet, a Gaussian, and a Lorentzian, which are attributed to paired protons, isolated and immobile protons, and mobile protons, respectively. For type I, on the other hand, the spectrum could not be simply interpreted as for types II–IV. In spite of this fact, we concluded, from naive insight without close examination of the possibility of the clustering, that the model for type I proposed by Slade *et al.* is favorable for interpretation of our results.

In the present paper, we report results of a close and quantitative examination of the various models, including the three-proton cluster model, by computer-simulation analyses of the lineshapes. It is needless to say that our main aim is to determine protonic locations in the bronzes. Contrary to the previous tentative conclusions, the results obtained in the present analyses indicate that, for type I, most ($\simeq$82%) of the intercalated hydrogens form the three-proton clusters, as proposed by Ritter *et al.*, and the others ($\simeq$18%) form pairs, as proposed by Slade *et al.* We also aim to determine the portion of each component of the spectra, because quantitative analyses have never carried out for the portion. It is demonstrated that the computer-simulation analysis of pulsed NMR spectra is a powerful tool for obtaining an information about the portion of various components.

Although our results support the excellent works done by Ritter *et al.*, their analyses were insufficient in the sense that (1) a uniaxial approximation was used in their calculation, and the interaction between spins at both ends was ignored, and (2) no examination was carried out for dependence of the spectra on the arrangement of the three protons. We therefore calculate the spectrum arising from the three-spin system without any approximations, and obtain the correct lineshape. The lineshape of the three-spin spectra is found to have strong dependence on the arrangement of the three spins and therefore, we can safely assign the lineshape to the arrangement.

## Experimental

All phases of the hydrogen molybdenum bronzes, type I ($H_{0.21}MoO_3$), type I ($H_{0.91}MoO_3$), type III ($H_{1.55}MoO_3$), and type IV ($H_{1.90}MoO_3$), were prepared by a method following Glemser and Lutz (*16*). Production of single phases has been proved with X-ray diffraction, infrared spectroscopy and Raman spectroscopy by the authors (*17, 18*). The samples comprised powders and were sealed in glass tubes to prevent decomposition.

Proton NMR were detected at liquid nitrogen temperature (77 K) and room temperature using a home-built pulsed NMR spectrometer operating at 11 MHz. Absorption spectra were obtained by Fourier transformation of FID (free induction decay) signals. Because the Fourier transform of the FID is usually distorted owing to the lack of the initial part of FID during the dead time of the receiver after an intense rf pulse, the lack was made up for by the corresponding part of the solid echo time domain signal using the center of the echo as time zero

(zero-time-resolution method (*19*)), where the solid echo signal is obtained by applying at 90° phase-shifted 90° pulse after the first 90° pulse. The signals with poor signal-to-noise ratio were accumulated and averaged to improve the signal-to-noise ratio.

The spectra for types I, II, III and IV observed at liquid nitrogen temperature are shown in Figs. 3a, 4a, 5a, and 6a, respectively. All of the spectra exhibit very broad background lines due to protons of water adsorbed in sample preparation. The spectrum of type I has three narrow peaks and deep dips at both sides of the central peak. The spectrum of type II is similar to that of type I, but the separation between side peaks is wider and the line is broader as compared with type I. In type III and IV, the whole lines are broader than that of type II. However, the widths of the central lines are narrower than that of type II. Details of the analyses for these spectra are discussed later.

## Theoretical

Before going into detailed analyses, we review the theoretical results used in the present analysis.

### *Isolated Protons*

The lineshapes of isolated and immobile protons and mobile protons are represented by the well known Gaussian and the Lorentzian formulas (*20*), respectively, as

$$G(f) = \frac{1}{\sqrt{2\pi}\,\Delta} e^{-f^2/2\Delta^2}, \tag{1}$$

and

$$L(f) = \frac{\delta}{\pi} \frac{1}{f^2 + \delta^2}. \tag{2}$$

### *Paired Protons*

As is well known the lineshape of the paired proton is called Pake-doublet (*21*) which is an NMR absorption line showing a splitting into two component lines due to the dipolar interaction between two spin-$\frac{1}{2}$ systems. In a single crystal, the two resonance lines are shifted from the resonance of bare nuclei by

$$f = \pm\alpha_D(3\cos^2\theta - 1), \tag{3}$$

where

$$\alpha_D = \frac{3\gamma^2 h}{4r^3}, \tag{4}$$

$\theta$ is the angle between an applied static magnetic field and the line joining the two spins, $\gamma$ is the gyromagnetic ratio, and $r$ is the distance between the two spins. Because the samples used in the present work comprise powders, $\theta$ distributes randomly over all of its available values. By integrating over all $\theta$ values, one can obtain the powder spectrum of the two-spin system as (*21*)

$$\begin{aligned} P(f) &= \left(-\frac{f}{\alpha_D} + 1\right)^{-1/2} \\ &\qquad \text{for } -2\alpha_D < f < -\alpha_D \\ &= \left(-\frac{f}{\alpha_D} + 1\right)^{-1/2} + \left(\frac{f}{\alpha_D} + 1\right)^{-1/2} \\ &\qquad \text{for } -\alpha_D < f < \alpha_D \\ &= \left(\frac{f}{\alpha_D} + 1\right)^{-1/2} \\ &\qquad \text{for } \alpha_D < f < 2\alpha_D. \end{aligned} \tag{5}$$

Actually, this spectrum is broadened by dipolar interactions with near spins without pairing. The observed spectrum can then be expressed as

$$D(f) = N\int_{-\infty}^{\infty} P(f')e^{-(f-f')^2/2\beta_D^2}\,df', \tag{6}$$

where $N$ is a normalization factor determined so that

$$\int_{-\infty}^{\infty} D(f)\,df = 1. \tag{7}$$

### *Three-Proton Cluster*

We consider the spectrum arising from the three-spin system illustrated in Fig. 1. In

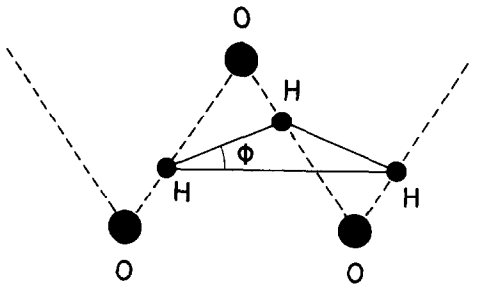


FIG. 1. Proton three-spin system in type I hydrogen molybdenum bronze. The angle $\phi = 22.2°$ gives the calculated spectrum best fitting the experimental one.

a single crystal, there are seven resonance lines of a three-spin system given as (22)

$$f = 0 \tag{8a}$$

$$f = \pm 2q \tag{8b}$$

$$f = \pm(3p + q) \tag{8c}$$

$$f = \pm(3p - q), \tag{8d}$$

where

$$p = \frac{1}{4}(A_{12} + A_{23} + A_{31})$$

$$q^2 = p^2 + r^2 + s^2$$

$$r = \frac{\sqrt{6}}{4}(A_{31} - A_{23})$$

$$s = \frac{\sqrt{2}}{4}(2A_{12} - A_{23} - A_{31})$$

$$A_{ij} = \frac{2\alpha_{ij}}{3}(3\cos^2\theta_{ij} - 1)$$

$$\alpha_{ij} = \frac{3\gamma^2 h}{4r_{ij}^3} = \alpha_T. \tag{9}$$

The transition probability of each line is given as (22)

$$w_0 = \frac{1}{8}\left(1 + \frac{3p^2}{q^2}\right)$$

$$w_{2q} = \frac{3}{16}\left(1 - \frac{p^2}{q^2}\right)$$

$$w_{3p+q} = \frac{1}{8}\left(1 + \frac{p}{q}\right)$$

$$w_{3p-q} = \frac{1}{8}\left(1 - \frac{p}{q}\right), \tag{10}$$

for (8a), (8b), (8c), and (8d), respectively The powder spectrum can be obtained b integrating the resonance lines (Eq. (8) multiplied by the weights (Eq. (10)) over al values of the azimuthal angle $\Omega$ as

$$T_0(f) = \frac{1}{4\pi}\int w_0(\Omega)\,\delta(f)\,d\Omega$$

$$T_{2q}(f) = \frac{1}{4\pi}\int w_{2q}(\Omega)[\delta(f - 2q) + \delta(f + 2q)]\,d\Omega$$

$$T_{3p+q}(f) = \frac{1}{4\pi}\int w_{3p+q}(\Omega)[\delta\{f - (3p + q)\} + \delta\{f + (3p + q)\}]\,d\Omega$$

$$T_{3p-q}(f) = \frac{1}{4\pi}\int w_{3p-q}(\Omega)[\delta\{f - (3p - q)\} + \delta\{f + (3p - q)\}]\,d\Omega. \tag{11}$$

The interactions of the three-spin systen with other spins result in a Gaussian broad ening;

$$T(f) = \int_{-\infty}^{\infty} G(f - f')[T_0(f') + T_{2q}(f') + T_{3p+q}(f') + T_{3p-q}(f')]\,df', \tag{12}$$

where

$$G(f - f') = \frac{1}{\sqrt{2\pi}\,\beta_T}\,e^{-(f-f')^2/2\beta_T^2}. \tag{13}$$

It should be noted that if the spectr would depend only weakly on the structur of the three-spin cluster, we could not assig the structure of the cluster to the observe spectra. In Fig. 2, we show the spectra o the three spin system calculated for severa angles $\phi$ of the isosceles triangle formed b the three spins. It is found, fortunately, tha the lineshape of the three-spin system de pends strongly on the angle $\phi$, so that w

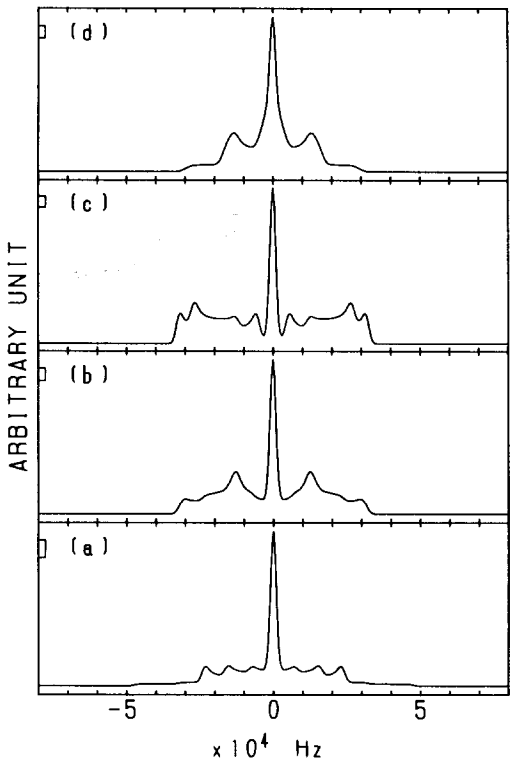


FIG. 2. Calculated Gaussian-broadened lineshapes of the three-spin system for several angles $\phi$ of the isosceles triangle as in Fig. 1. The angles $\phi$ are equal to (a) 0°, (b) 30°, (c) 60°, and (d) 75°.

could safely assign the structure of the three spin system to observed lineshape.

We also examined the approximation used in Ref. (*13*). In a case that the cluster of spins 1, 3, and 2 (in Fig. 8 of Ref. (*13*)) can be approximated by line (uniaxial approximation) with equal separation, $s$ and $q$ in Eq. (9) are expressed as

$$s = -\frac{14\sqrt{2}}{17}p,$$

$$q = \frac{\sqrt{681}}{17}p. \qquad (14)$$

If we neglect the interaction between spins 1 and 2 at both ends, $q$ is given by

$$q = \sqrt{3}p. \qquad (15)$$

The spectra calculated within the above two approximations indicated that both of uniaxial approximation and an omission of the interaction cannot give the correct lineshape for $\phi \geqq 15°$.

## Analyses

In this section, we present the procedure and the results of our analyses for the experimental spectra. As was mentioned before, the spectra show very broad lines arising from protons in adsorbed water. We subtract the broad line component in analyses.

### *Type I*

In type I Dickens *et al.* (*4, 5*) detected OH groups using inelastic neutron scattering (INS). The lineshape observed in the present experiment shows the deep dips at both sides of the central peak. We first tried to interpret the lineshape by a superposition of a Pake-doublet, a Gaussian and a Lorentzian, as in the cases of types II–IV (see below). However, no simulated spectra composed of the above three components could fit the observed one. In particular, the deep dips could not be reproduced by any Pake-doublets.

The next candidate to be considered is the three proton clusters proposed by Ritter *et al.* (*13, 14*). We have calculated the spectra arising from the three spin systems illustrated in Fig. 1 and obtained a fairly good agreement with observed ones. The spectrum of type I observed in the present work, however, could not be fully interpreted in terms of only the three-spin systems. Therefore it is natural to consider the protons forming pairs in part. The spectrum in this case is interpreted as a superposition of a Pake-doublet $D(f)$ (Eq. (6)) and a three-spin spectrum $T(f)$ (Eq. (12)) as

$$Z(f) = a \cdot D(f) + d \cdot T(f). \qquad (16)$$

A simulated spectrum best fitting the ex-

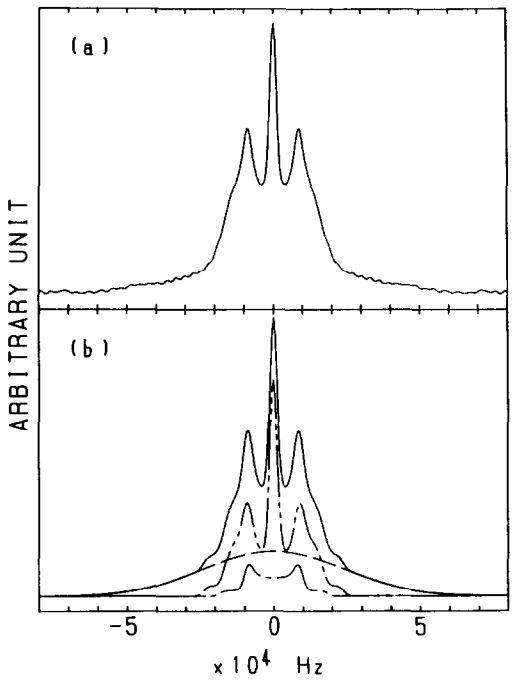


FIG. 3. (a) Experimental and (b) simulated lineshapes of proton NMR spectrum in type I. Component lines are displayed together, where the line having three peaks (———) is the one arising from three spin system and the one having two peaks (———) is the Pake-doublet. The very broad line (———) is due to protons in adsorbed water.

perimental one was obtained by varying the parameters $\alpha_D$ and $\beta_D$ in Eq. (6), $\alpha_T$ and $\beta_T$ in Eq. (12), and by determining the coefficients $a$ and $d$ in Eq. (16), together with the broad background component, by the least square method.

As shown in Fig. 3, the spectrum of type I can be successfully expressed by Eq. (16) calculated by assuming the angle $\phi$ of the isosceles triangle formed by the three spins to be 22.2° (Fig. 1). Determined coefficients $a$ and $d$ are listed in Table I, from which it is found that most protons (≃82%) form the three spin system and remaining ones (≃18%) form the two-spin system in $MoO_3$ layers of type I. There are little isolated or moving protons in type I. The distance $r$ of the nearest neighbor protons determined from $\alpha_D$ and that from $\alpha_T$ are same as each other and found to be 0.21 nm, which agree well with the value obtained by Dickens *et al.* (*4*).

*Types II, III, and IV*

Dickens *et al.* (*4*) detected $OH_2$ groups in types II–IV at 77 K using INS. One expects from the existence of $OH_2$ groups that the spectrum of protons should exhibit the Pake-doublet (*21*). Besides the paired protons, there would be isolated ones fixed in position, or moving in or between the layers (*14*). Then we assume for types II–IV that the lineshape of the spectrum is a superposition of a Pake-doublet $D(f)$ (Eq. (6)), a Gaussian $G(f)$ (Eq. (1)), and a Lorentzian $L(f)$ (Eq. (2)). The Gaussian lineshape is due to fixed protons and the Lorentzian to moving ones (*20*).

The superposition of three lines can be expressed as

$$Y(f) = a \cdot D(f) + b \cdot G(f) + c \cdot L(f). \quad (17)$$

For types II–IV, the parameters $\alpha_D$ and $\beta_D$ in Eq. [6], $\Delta$ in Eq. (1) and $\delta$ in Eq. (2) were varied, and coefficients $a$, $b$, and $c$ in Eq. (17) were determined by the same method as used in the case of type I.

In Figs 4–6, excellent agreements between experimental and simulated lineshapes are demonstrated. Coefficients determined by the simulation are listed in Table I, and proton–proton distance $r$ is calculated to be 0.15 nm in these three phases. The closer distance indicates the existence of hydrogen pairs $OH_2$, which is consistent with INS detection by Dickens *et al.* In types II–IV, most of protons forms pairs and remaining ones are isolated and immobile or are moving between $MoO_3$ layers.

*Transition of Protonic Structure*

In Fig. 7, we plot the portion of each component obtained in the present analyses

TABLE I

FITTING PARAMETERS $\Delta$, $\delta$, $\alpha_D$, $\beta_D$, $\alpha_T$, AND $\beta_T$ (in kHz) USED IN THE ANALYSES, HYDROGEN CONTENTS $a$, $b$, $c$, AND $d$ (in %) OF DIFFERENT LOCATIONS, AND DISTANCES $r$ (in nm) BETWEEN NEAREST NEIGHBOR PROTONS, DETERMINED BY THE SIMULATION ANALYSES

| Type | $\Delta$ | $\delta$ | $\alpha_D$ | $\beta_D$ | $\alpha_T$ | $\beta_T$ | $a$ | $b$ | $c$ | $d$ | $r$ |
|---|---|---|---|---|---|---|---|---|---|---|---|
| I | — | — | 9.3 | 1.3 | 9.3 | 1.3 | 18 | — | — | 82 | 0.21 |
| II | 6.2 | 3.5 | 26 | 6.2 | — | — | 71 | 17 | 12 | — | 0.15 |
| III | 7.2 | 0.8 | 26 | 7.2 | — | — | 84 | 14 | 2 | — | 0.15 |
| IV | 9.2 | 0.7 | 28 | 9.2 | — | — | 62 | 32 | 6 | — | 0.15 |

against proton content $x$. This figure clearly indicates the transition of the protonic structure from three-proton clusters in type I to proton pairs in type II.

## Discussion

In this section, we estimate the proton/Mo ratio $x$ around which the above transition takes place, from the view point of stability of protonic distribution.

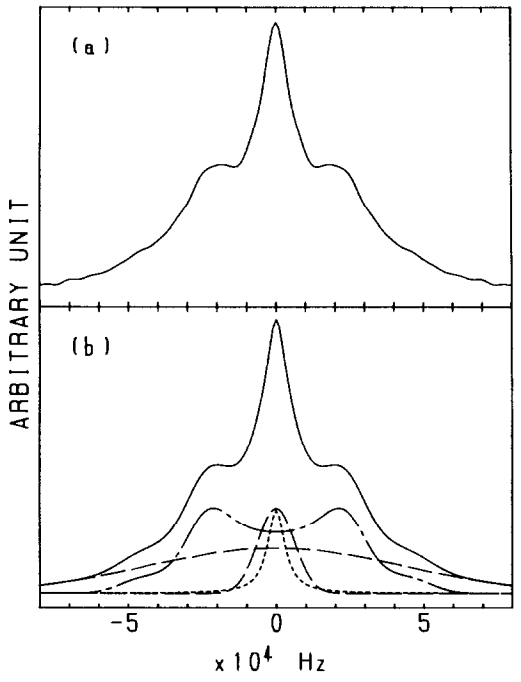


FIG. 4. (a) Experimental and (b) simulated lineshapes of proton NMR spectrum in type II. Component lines are displayed together, where the line having two peaks (————) is the Pake-doublet, the broader one (———) the Gaussian and the narrower one (---------) the Lorentzian. The very broad line (———) is due to protons in adsorbed water.

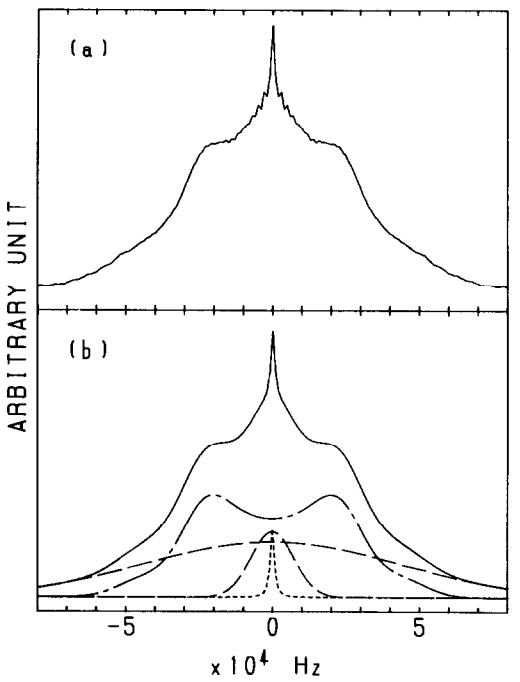


FIG. 5. (a) Experimental and (b) simulated lineshapes of proton NMR spectrum in type III. Component lines are displayed together, where the line having two peaks (————) is the Pake-doublet, the broader one (———) the Gaussian, and the narrower one (---------) the Lorentzian. The very broad line (———) is due to protons in adsorbed water.

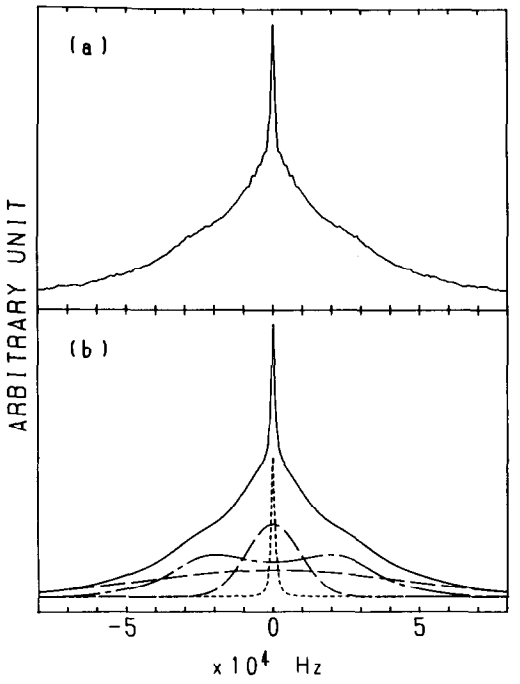


FIG. 6. (a) Experimental and (b) simulated lineshapes of proton NMR spectrum in type IV. Component lines are displayed together, where the line having two peaks (—·—·—) is the Pake-doublet, the broader one (———) the Gaussian, and the narrower one (·····) the Lorentzian. The very broad line (———) is due to protons in adsorbed water.

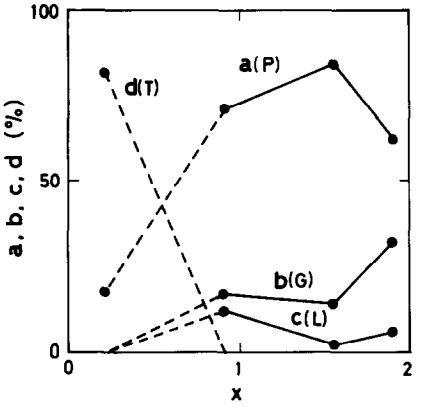


FIG. 7. Plots of the portions (in %) of each component versus hydrogen content $x$: (a) paired protons, (b) immobile isolated protons, (c) mobile isolated protons, (d) three proton clusters.

When three-proton clusters occupy their all available positions on the zigzag chains of intralayer oxygen atoms as shown in Fig. 8a, the value of $x$ is 0.67. Although three-proton clusters could occupy the available positions of other chains (dotted lines and circles) facing the original ones, one proton of the three-proton clusters on these chains is too close for this location to be stable. On the other hand, when three-proton clusters are located alternatively on their available positions (Fig. 8b), the value of $x$ is 0.43. This insertion manner of protons would be more stable than the above. Then, insertion manners of three proton clusters with less $x$'s should be more stable in type I.

With respect to paired protons inserted in types II, the value of $x$ of possible maximum insertion, as shown in Fig. 8c, is 1.0. However, in type II, the configuration in which all protons occupy available positions on the same sides of the zigzag

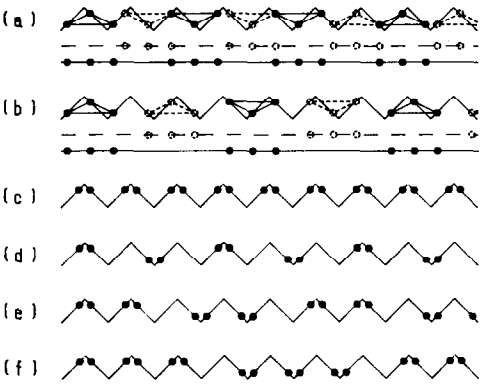


FIG. 8. Models for the distribution of protons; (a) $x = \frac{12}{18} = 0.67$ and (b) $x = \frac{6}{14} = 0.43$ for three-proton clusters; (c) $x = \frac{2}{2} = 1$, (d) $x = \frac{4}{6} = 0.67$, (e) $x = \frac{8}{10} = 0.8$, and (f) $x = \frac{12}{14} = 0.86$ for paired protons.

chain should be unstable. Stable configurations expected are shown in Figs. 8d, e, and f. The values of $x$ are 0.67, 0.80, and 0.86 for the configurations in Figs. 8d, 8e, and 8f, respectively. Therefore, these configurations are very reasonable in type II and combinations of these configurations are expected to exist.

Another insertion manners could exist for higher values of $x$ than the above in type II and in types III and IV, so that protons are inserted on the zigzag chains of interlayer oxygen atoms.

Above consideration, together with discussion about the lattice constant and the activation energy in the previous paper (*15*), clearly supports that the transition of the protonic structure takes place from three proton clusters in type I to paired protons in type II.

## Conclusions

NMR lineshapes for all four types of $H_xMO_3$ are obtained by using pulsed NMR. The method used in the present study can yield various information and is a powerful tool. We determine the locations of protons in all four types by computer-simulation analyses of the lineshapes. Our analyses show that protons in type I form three-proton clusters and paired protons, whereas those in types II–IV form paired protons, isolated and immobile ones, and mobile ones. The portion of each component were determined for all four types of $H_xMO_3$. We also deduced other information related to protonic structure and transition.

## References


1. For a recent example: S. P. MEHANDRU AND A. B. ANDERSON, *J. Am. Chem. Soc.* **110,** 2061 (1988).
2. J. J. BIRTILL AND P. G. DICKENS, *Mater. Res. Bull.* **13,** 311 (1978).
3. N. SOTANI, Y. KAWAMOTO, AND M. INUI, *Mater. Res. Bull.* **18,** 797 (1983).
4. P. G. DICKENS, J. J. BIRTILL, AND C. J. WRIGHT, *J. Solid State Chem.* **28,** 185 (1979).
5. P. G. DICKENS, S. J. HIBBLE, AND G. S. GAMES, *Solid State Ionics* **20,** 213 (1986).
6. P. G. DICKENS, A. T. SHORT, AND S. CROUCH-BAKER, *Solid State Ion. React.* **28–30,** 1297 (1988).
7. R. C. T. SLADE, P. R. HIRST, B. C. WEST, R. C. WARD, AND A. MAGERL, *Chem. Phys. Lett.* **155,** 305 (1989).
8. R. C. T. SLADE, P. R. HIRST, AND H. A. PRESSMAN, *J. Mater. Chem.* **1,** 429 (1991).
9. A. CIRILLO AND J. J. FRIPIAT, *J. Phys. (Paris)* **39,** 247 (1978).
10. A. C. CIRILLO, JR., L. RYAN, B. C. GERSTEIN, AND J. J. FRIPIAT, *J. Chem. Phys.* **73,** 3060 (1980).
11. R. E. TAYLOR, M. M. SILVA CRAWFORD, AND B. C. GERSTEIN, *J. Catal.* **62,** 401 (1980).
12. R. C. T. SLADE, T. K. HALSTEAD, AND P. G. DICKENS, *J. Solid State Chem.* **34,** 183 (1980).
13. CL. RITTER, W. MÜLLER-WARMUTH, H. W. SPIESS, AND R. SCHÖLLHORN, *Ber. Bunsenges. Phys. Chem.* **86,** 1101 (1982).
14. CL. RITTER, W. MÜLLER-WARMUTH, AND R. SCHÖLLHORN, *J. Chem. Phys.* **83,** 6130 (1985).
15. N. SOTANI, K. EDA, AND M. KUNITOMO, *J. Chem. Soc. Faraday Trans.* **86,** 1583 (1990).
16. O. GLEMSER AND G. LUTZ, *Z. Anorg. Allg. Chem.* **264,** 17 (1951).
17. K. EDA, *J. Solid State Chem.* **83,** 292 (1989).
18. N. SOTANI, K. EDA, M. SADAMATU, AND S. TAKAGI, *Bull. Chem. Soc. Jpn.* **62,** 903 (1989).
19. J. G. POWLES AND J. H. STRANGE, *Proc. Phys. Soc. London,* **82,** 6 (1963).
20. A. ABRAGAM, "The Principles of Nuclear Magnetism," Oxford, London (1961).
21. G. E. PAKE, *J. Chem. Phys.* **16,** 327 (1948).
22. E. R. ANDREW AND R. BERSOHN, *J. Chem. Phys.* **18,** 159 (1950).